Phonons and defects in semiconductors and nanostructures: Phonon trapping, phonon scattering, and heat flow at heterojunctions

S. K. Estreicher,[a] T. M. Gibbons, By. Kang, and M. B. Bebek
Physics Department, Texas Tech University, Lubbock, Texas 79409-1051, USA

(Received 8 July 2013; accepted 5 September 2013; published online 2 January 2014)

Defects in semiconductors introduce vibrational modes that are distinct from bulk modes because they are spatially localized in the vicinity of the defect. Light impurities produce high-frequency modes often visible by Fourier-transform infrared absorption or Raman spectroscopy. Their vibrational lifetimes vary by orders of magnitude and sometimes exhibit unexpectedly large isotope effects. Heavy impurities introduce low-frequency modes sometimes visible as phonon replicas in photoluminescence bands. But other defects such as surfaces or interfaces exhibit spatially localized modes (SLMs) as well. All of them can trap phonons, which ultimately decay into lower-frequency bulk phonons. When heat flows through a material containing defects, phonon trapping at localized modes followed by their decay into bulk phonons is usually described in terms of phonon scattering: defects are assumed to be static scattering centers and the properties of the defect-related SLMs modes are ignored. These dynamic properties of defects are important. In this paper, we quantify the concepts of vibrational localization and phonon trapping, distinguish between normal and anomalous decay of localized excitations, discuss the meaning of phonon scattering in real space at the atomic level, and illustrate the importance of phonon trapping in the case of heat flow at Si/Ge and Si/C interfaces. © *2014 AIP Publishing LLC*. [http://dx.doi.org/10.1063/1.4838059]

I. INTRODUCTION

Optical techniques, such as Fourier-transform infrared (FTIR) absorption, Raman, or photoluminescence (PL), have been used for decades to identify and characterize impurities in semiconductors. In the case of light impurities such as H (Ref. 1) or O (Ref. 2) in Si, a number of high-frequency local vibrational modes (LVMs) are measured by FTIR and/or Raman and predicted by theory. Heavier impurities such as transition metals often give rise to PL spectra, which exhibit sharp phonon sidebands,[3] indicative of low-frequency pseudo-local modes associated with the defect. Such low-frequency modes are difficult to identify.[4]

However, all defects produce localized vibrational modes, many of which cannot be seen by traditional experimental techniques because they are within a phonon band of the host crystal, have short lifetimes, or other practical reasons. Defect-related vibrational modes are localized in space, in contrast to bulk modes which involve the oscillation of many atoms in the crystal.

The degree of localization of a vibrational mode can be quantified using the eigenvectors of the dynamical matrix of the system. In this paper, we call spatially localized mode (SLM) any defect-related vibrational mode that exhibits a substantial degree of spatial localization around the defect. This is a broader definition than the usual LVM which applies to IR- or Raman-active high-frequency modes of light impurities. While LVMs are understood to be isolated in frequency, SLMs are localized in space as only a few atoms at or near the defect oscillate.

The vibrational lifetimes τ of many high-frequency LVMs have been measured by transient-bleaching spectroscopy[5–7] or estimated from their low-temperature IR line width.[8] The data show that some Si-H stretch mode excitations survive for hundreds of picoseconds (ps) while others decay in just a few ps.[6] Further, isotope substitutions which result in very small frequency shifts sometimes cause huge changes in vibrational lifetime.[7,8] First-principles theory has explained many of these results.[7–9]

These experimental data and theoretical studies imply that all defects trap phonons. While it is well known that some defects can trap small amounts of electric charge, the fact that they also trap small amounts of energy is not yet fully appreciated. The energy remains localized at/near the defect for the length of time τ, which can vary from a few to a few hundred ps depending on the defect and sometimes its isotopic composition.

In a few cases, the conventional theory[10,11] of an isolated high-frequency excitation coupled to a low-frequency phonon bath explains the data, and then the vibrational lifetimes are mostly isotope-independent. We call such decays *normal*. But in many cases, the lifetimes are not only much shorter than expected but sometimes extraordinarily sensitive to the isotopic composition of the defect. We label such decays *anomalous*.

In terms of heat flow, phonon trapping is not of great consequence for high-quality bulk crystals in which typical defect concentrations are in the parts-per-million range. In this limit, the impact of defects on the flow of heat is well described in terms of (bulk) phonon scattering.[12] But when the defect concentration is in the atomic percent range (as is often the case in nanostructures) or is locally high (as is the case at heterojunctions), phonon trapping affects the flow of

[a]Author to whom correspondence should be addressed. Electronic mail: Stefan.Estreicher@ttu.edu

heat in a substantial way and the defect-related SLMs should be explicitly included in the description of the process. Finally, when the defect concentration is very high—the amorphous or alloy limit—the defect-related modes are no longer strongly localized but form bands. This limit is not addressed in this paper.

This paper begins (Sec. II) with an overview of the theoretical approach used to calculate vibrational lifetimes, decay modes, and perform the non-equilibrium *ab-initio* molecular-dynamics (MD) simulations we use to study heat flow in semiconductors. In Sec. III, we quantify the localization of defect-related vibrational modes and show that all defects introduce high- and/or low-frequency SLMs. Some of them can only be excited optically, but most can be excited thermally as well. Section IV focuses on the normal or anomalous decay of high- and low-frequency vibrational excitations. In Sec. V, we describe the empirical concept of (bulk) phonon scattering by defects as phonon trapping followed by (normal or anomalous) decay. In Sec. VI, we examine the consequences of these processes on the flow of heat through a monoatomic δ layer and at the interface between two materials. The key points are summarized in Sec. VII.

II. KEY INGREDIENTS OF THE THEORETICAL APPROACH

All the theoretical predictions in this paper are obtained using "first-principles" type calculations.[13] The host crystal is represented by 3D- or 1D-periodic supercells containing up to a few hundred atoms. The nuclei obey classical laws of motion with forces obtained from total energies via the Hellmann-Feynman theorem.[14] The electronic regions near the atomic cores are replaced by *ab-initio*-type pseudopotentials, and the electronic valence regions are described with density-functional theory. We use the SIESTA method[15] with pseudo-atomic (numerical) basis sets for the valence states, but plane-wave or all-electron codes produce the same results.[16] The details of our calculations (basis sets, pseudopotentials, exchange-correlation potential, etc.) are discussed in Refs. 9 and 16. In this paper, we use results obtained earlier as well as unpublished results. The supercells range from the 3D-periodic Si_{64} cell to a 1D periodic $Si_{200}H_{32}$ nanowire; the basis sets are double-zeta for the first two rows of the Periodic Table with polarization function for the 3rd row and below; we use the local-density approximation in most calculations and the generalized gradient approximation when heavier elements are involved.

The key ingredient of the calculations is the dynamical matrix, calculated at $k = 0$. It needs to be accurate (no negative eigenvalues): the supercell and then the defect geometry must be carefully optimized. The eigenvalues of this matrix are the normal-mode frequencies ω_s of the system. The ortho-normal eigenvectors $e_{\alpha i}{}^s$ give the relative displacement of atom α along $i = x, y, z$ in the normal mode s. The temperature (T) and time (t) dependence of the Cartesian coordinates $r_{\alpha i}{}^s$ are related to these eigenvectors via q_s, the normal-mode coordinate: $r_{\alpha i}{}^s(T,t) = q_s(T,t)\, e_{\alpha i}{}^s$.

The simplest way to prepare the supercell in thermal equilibrium at $t = 0$ is to assume that the modes are approximately harmonic, that is $q_s(T,t) \approx A_s(T) \cos(\omega_s t + \varphi_s)$. This introduces a random distribution of phases φ_s. Note that the non-equilibrium MD simulations do not assume harmonicity, since the atomic displacements are calculated using forces derived from total energies at every time step. The unknown amplitudes $A_s(T)$ are obtained by requiring that, in thermal equilibrium, the average energy of each mode is k_BT. This introduces a random set of mode energies since this condition only applies to the *average* mode energies.[9,16] Therefore, the MD simulations need to be repeated over many sets of random initial mode phases and energies. The time step in the MD run is 1/40th–1/30th of the fastest oscillation in the system, typically 1 fs if the system includes C-Si, Si-S, and/or Ge-Si bonds, but at most 0.5 fs if H-Si bonds are also involved.

No thermostat can be used since it would artificially force the system back into thermal equilibrium much faster than the various vibrational modes actually couple. However, no thermostat is needed because our supercell preparation method produces a system very close to thermal equilibrium and the temperature fluctuations are remarkably small, especially after averaging.

Thus, the ortho-normal eigenvectors of the dynamical matrix are very precious as they are used to (i) prepare (parts of) the supercell in thermal equilibrium at a desired temperature; (ii) add $3\hbar\omega/2$ potential energy (zero-point energy plus one phonon) to a specific vibrational mode at $t = 0$; (iii) convert a set of 3N Cartesian coordinates obtained from a MD simulations into a linear combination of the 3N normal vibrational modes of the system. This allows us to monitor the energy and amplitude of the decaying mode and sometimes identify the receiving modes; (iv) quantify the localization of specific modes on an atom or a group of atoms.

There are several advantages in our supercell preparation over the conventional random distribution of velocities followed by lengthy thermalization runs. First, there is no need to do any thermalization run and the supercell is almost in perfect thermal equilibrium at step 1. Second, supercell preparation leads to temperature fluctuations (without thermostat) that are very much smaller than can be achieved with conventional thermalization, even with a thermostat and after tens of thousands of time steps (see, e.g., Fig. 1 in Ref. 9 or Fig. 2 in Ref. 16). For example, we can easily monitor temperature changes from 120 K to 125 K, especially after averaging. Temperature control is essential because the vibrational lifetimes drop fast as T increases. Third, we can prepare the supercell slightly away from equilibrium in a controlled manner and monitor how it returns to equilibrium, without thermostat. This cannot be achieved with conventional thermalization.

Note that this supercell preparation and the subsequent non-equilibrium MD runs can be done with any theoretical method, even with empirical potentials. We use first-principle methods which do not contain empirical parameters such as coupling constants between selected vibrational modes. Our density-functional-based method includes *ab-initio* pseudopotentials for the core regions and local basis sets in the valence regions (SIESTA). However, we have tested it with an all-electron code (no pseudopotentials), and

others have used empirical potentials, as well as a plane-wave based code. The key is to have an accurate dynamical matrix.

III. BULK AND SPATIALLY LOCALIZED MODES

In this paper, the normal vibrational modes of the unperturbed host crystal are called "bulk". In equilibrium, these atomic vibrations spread over most of the host atoms in the system and the magnitude of the oscillation of any one atom is very small. If a temperature gradient is applied, bulk phonons transport heat from the warmer to the colder parts of the crystal. When defects are present, most bulk modes remain bulk in nature but a number of SLMs are introduced. They involve the oscillations of a small number of atoms in the immediate vicinity of the defect.

The localization[17] of a SLM can be quantified using the eigenvectors dynamical matrix. Since $e_{\alpha i}^{s}$ gives the relative displacement of atom α in the direction $i = x, y, z$ for the normal mode s, the sum over all the atoms in the system gives 1 (i.e., $\Sigma_\alpha L_\alpha^2 = 1$). The localization of mode s on the (group of) atom(s) α is $L_\alpha^2 = (e_{\alpha x}^{s})^2 + (e_{\alpha y}^{s})^2 + (e_{\alpha z}^{s})^2$ with $0 \leq L_\alpha^2 < 1$. The plot of $L_\alpha^2(\omega)$ shows the localization of all the modes on the atom(s) α.

Figure 1 shows $L_\alpha^2(\omega)$ calculated for interstitial oxygen (O_i) in Si. If α stands for oxygen, the asymmetric stretch at 1187 cm^{-1} has $L_O^2 \approx 0.80$ and two low-frequency wag-type modes at 86 and 224 cm^{-1} both have $L_O^2 \approx 0.20$. If α stands for the two silicon nearest neighbors (NNs) to O_i, the asymmetric stretch of O_i at 1187 cm^{-1} has $L_{Si}^2 \approx 0.20$. The symmetric Si-Si stretch mode at 641 cm^{-1} ($L_{Si}^2 \approx 0.95$) and the wag-type modes at 537 cm^{-1} ($L_{Si}^2 \approx 0.40$) involve no O_i motion at all.

Figures 2 and 3 show $L_\alpha^2(\omega)$ for the atoms at a Si/C and Si/Ge interface, respectively, in a δ-doped Si nanowire.[18] The Si-C and Si-Ge interface bonds are associated with many SLMs, some of which exhibit a substantial degree of localization. Note that most C-related modes have frequencies above $\sim$700cm^{-1} while all the Ge-related SLMs have frequencies below $\sim$300cm^{-1}. At room temperature, nearly all the Ge modes are excited but almost none of the C-related ones are.

Defect-related SLMs can be excited optically and/or thermally depending on their frequency. This leads to the

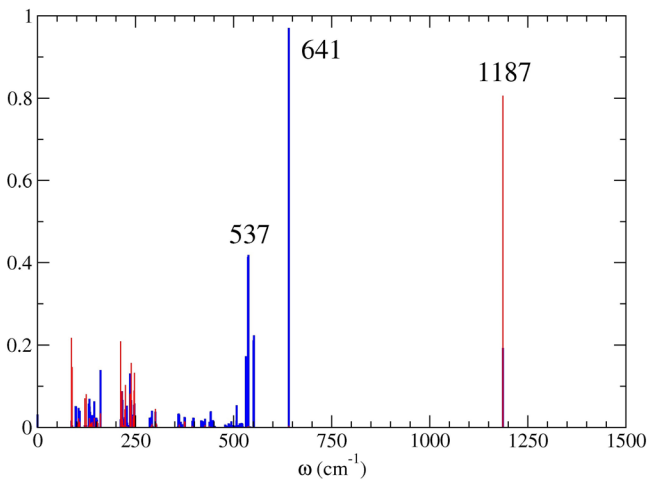

FIG. 1. SLMs associated with O_i in Si. The displacements of O_i are in red and those of its two Si NNs are in blue.

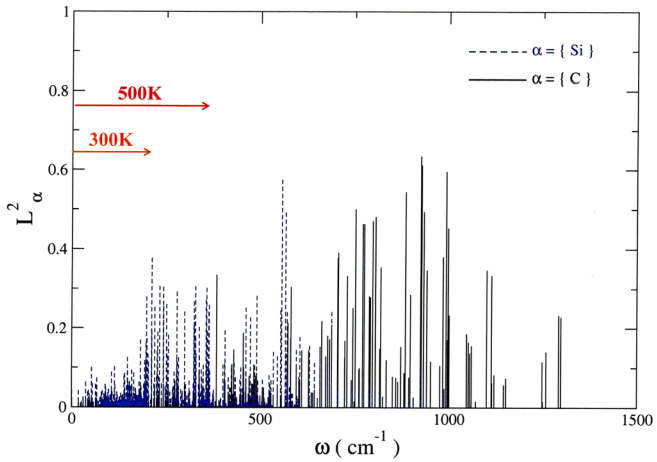

FIG. 2. SLMs associated with the Si/C interface in a C δ-doped Si nanowire. The Si displacements are in blue (dashed lines) and those of C are in black (solid lines). The "300K" and "500 K" arrows show the range of thermal phonons at the specified temperature.

localization of phonons at the defect, a phenomenon called *phonon trapping*.[19] A trapped phonon ultimately decays into a combination of lower-frequency bulk phonons. Its lifetime varies substantially with the defect and sometimes its isotopic composition, but does not necessarily correlate with its frequency.

IV. NORMAL AND ANOMALOUS DECAY

Direct measurements of the vibrational lifetimes of high-frequency IR-active LVMs using transient bleaching spectroscopy[5–7] require sub-ps pulses of a tunable laser. The lifetimes can also be estimated from the IR line width at low temperatures.[8] The lifetimes of several dozen high-frequency H-, D-, and O-related stretch modes and, in some cases, their temperature and/or isotope dependence have been measured[5–7] and calculated.[7–9] In a few cases, the temperature-dependence of the decay is consistent with the theory of Nitzan[10] and Egorov[11] which describes the

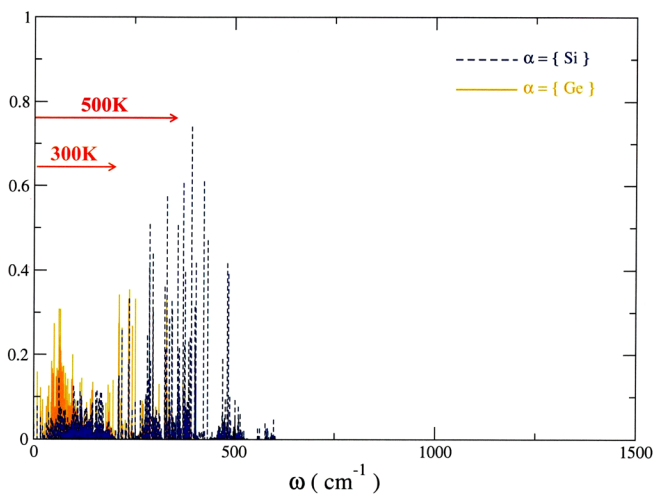

FIG. 3. SLMs associated with the Si/Ge interface in a Ge δ-doped Si nanowire. The Si displacements are in blue (dashed lines) and those of Ge are in gold (solid lines). The "300K" and "500K" arrows show the range of thermal phonons at the specified temperature.

coupling of a high-frequency mode to a low-frequency phonon bath (normal decay). But in most cases, the lifetime is considerably shorter than expected and surprisingly large isotope effects are observed (anomalous decay).

An example of normal decay is the 2072 cm^{-1} Si-H stretch mode of V_2H_2 in Si (a divacancy with two hydrogen atoms). This lifetime is very long, $\tau = 291 \pm 4$ ps at low temperatures, consistent with the predicted five-phonon process.[6] Thus, the optical excitation of the Si-H stretch mode at 2072 cm^{-1} results in the trapping by V_2H_2 of $\hbar\omega$(Si-H) = 0.26 eV for 291 ps at low temperatures (this lifetime drops to ~100 ps at room temperature).

Figure 4 shows the calculated (at T = 0) phonon density of states (pDoS) of Si and the localization of the modes of V_2H_2. A phonon trapped in the (calculated) 2 083 cm^{-1} mode decays into a combination of bulk phonons. Indeed, the two sets of H wag modes (doublets) at 597 cm^{-1} involve H motion perpendicular to the Si-H axis and no momentum transfers in first order. The Si-related modes at 585 cm^{-1} do not couple because the ratio of the 2 083 and 585 frequencies is about 3.5, an impossible number of phonons. The only other LVMs associated with V_2H_2 are the weakly localized modes around 182 cm^{-1} associated with the six Si NNs to the divacancy. But their amplitudes do not increase during the decay of the 2083 cm^{-1} mode.

An example of anomalous decay is give by the 2 062 cm^{-1} Si-H stretch mode of the H_2^* defect in Si. This defect consists of one Si-Si bond replaced by two Si-H bonds along the trigonal axis of the crystal, with one H at an antibonding (ab) and the other at a bond-centered (bc) site: H_{ab}–Si···H_{bc}–Si. The frequency of the H_{bc}–Si stretch mode is at 2 062 cm^{-1} is very close to the 2 072 cm^{-1} of V_2H_2. But its low-temperature vibrational lifetime, $\tau = 4.2 \pm 0.2$ ps, is almost 100 times shorter than that of V_2H_2. Yet, the fit of its temperature dependence to conventional theory[10,11] predicts that its decay should be a very slow 6-phonon process.[6] Something else is going on.

Figure 5 shows the localization of the modes associated with the H_2^* defect. There are two Si-H stretch modes along

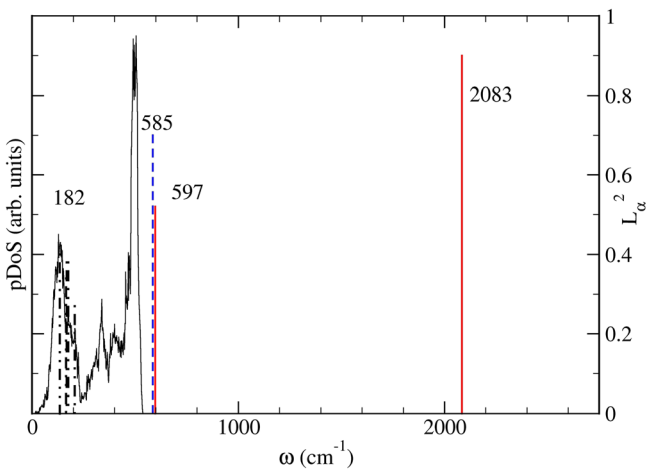

FIG. 4. Calculated pDoS of Si (left scale) and SLMs associated with the V_2H_2 defect (right scale). The excitation of the stretch mode at 2 083 cm^{-1} decays into five or more bulk phonons. Neither the H wag modes at 585 cm^{-1} nor the Si-related modes at 597 and 182 cm^{-1} participate in the decay (see text).

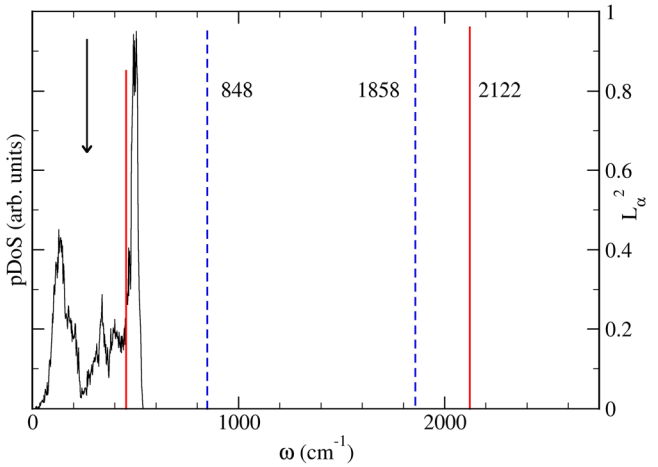

FIG. 5. Calculated pDoS of Si (left scale) and SLMs associated with the H_2^* defect. The excitation of the H_{bc}–Si stretch mode at 2122 cm^{-1} decays into the lower-frequency H_{ab}–Si stretch mode at 1 858 cm^{-1} plus the Si-Si symmetric stretch at 264 cm^{-1} (long vertical arrow). The 848 and 455 cm^{-1} modes are the H wag modes associated with H_{bc}–Si and H_{ab}–Si, respectively. Their amplitudes do not increase during the decay of the 2 122 cm^{-1} mode.

the same trigonal axis. MD simulations[9] show that the H_{bc}–Si stretch (calculated at 2 122 cm^{-1}) decays into the H_{ab}–Si stretch (calculated at 1 858 cm^{-1}) plus the weakly localized symmetric stretch of the two Si atoms in the defect (calculated at 264 cm^{-1}, arrow). Thus, the decay is a two-phonon process, consistent with a ~4 ps lifetime. It involves no bulk phonon at all, explaining why conventional theory fails.

After the H_{bc}–Si stretch mode has decayed, a phonon is still trapped in the H_{ab}–Si stretch mode and a second one in the Si–Si symmetric stretch mode. The decay of H_{ab}–Si has been predicted[9] to involve H wag modes with a lifetime estimated at 3.4 ps.[20] The lifetime of the Si–Si stretch is not known but is expected to be very short. Thus, the optical excitation of the Si-H stretch mode at 2 062 cm^{-1} results in the trapping by H_2^* of $\hbar\omega$(Si-H_{bc}) = 0.26 eV for 4 ps, and then of $\hbar\omega$(Si-H_{ab}) = 0.23 eV for 3.4 ps and $\hbar\omega$(Si-Si) = 0.03 eV for a short time. Thus, H_2^* traps about 0.25 eV for a total of about 8 ps while V_2H_2 traps the same amount of energy for almost 300 ps.

An example of huge isotope effect involves one of the two configurations of the H_2^*(C) defect in Si.[8] It has two H interstitials trapped at substitutional C atom: H_{ab}–C···H_{bc}–Si. Thus, H_2^*(C) is very similar to H_2^* with one Si replaced by C. The broad IR line width of the H_{ab}–C stretch mode of H_{ab}–C···H_{bc}–Si at 2 688.3 cm^{-1} gives a 2.4 ps lifetime, but the narrow line width of the H_{ab}–C stretch mode of H_{ab}–C···D_{bc}–Si at 2 688.6 cm^{-1} gives a 39 ps lifetime. Thus, upon D substitution, the frequency of the H_{ab}–C stretch mode shifts by 0.3 cm^{-1} (0.01% change) while the lifetime increases by a factor of 16 (1 625% change).

Theory shows that in H_{ab}–C···H_{bc}–Si, the excitation of the H_{ab}–C stretch mode at 2567 cm^{-1} (calculated) decays via the H_{bc}–Si stretch mode at 2183 cm^{-1} plus a bulk phonon at 384 cm^{-1} (Fig. 6), a two phonon decay. When H_{bc}–Si is substituted with D_{bc}–Si, the frequency of the H_{ab}–C stretch mode remains virtually unchanged at 2564 cm^{-1} (calculated), but that of the receiving D_{bc}–Si mode drops to

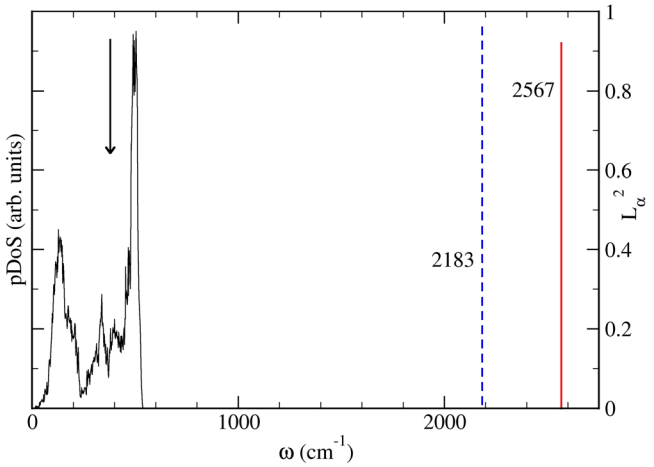

FIG. 6. Calculated pDoS of Si (left scale) and localization (right scale) of the H_{ab}–C stretch mode at 2 567 cm^{-1} and of the receiving H_{bc}–Si stretch mode at 2 183 cm^{-1}. The arrow points to $\Delta\omega$, with $\hbar\omega(H_{ab}\text{-}C) = \hbar\omega(H_{bc}\text{-}Si) + \hbar\Delta\omega$.

1 567 cm^{-1}. Now, two bulk phonons are needed to make up for the missing 997 cm^{-1} (Fig. 7), leading to a three-phonon decay.[8]

No experimental information is available on low-frequency SLMs. They are difficult if not impossible to see using FTIR. However, the theoretical method used to calculate the lifetimes of high-frequency modes can be used for low-frequency SLMs as well as for bulk modes. All we need to do is use the appropriate eigenvector of the dynamical matrix to add $3\hbar\omega/2$ potential energy to the vibrational mode in a supercell in thermal equilibrium at the temperature T. Then, we perform non-equilibrium *ab-initio* MD simulations and monitor the energy and amplitude of the excited mode as a function of time. Identifying the decay channels can be difficult because all the low-frequency modes we have studied so far exhibit normal decays with two or more decay channels.[21]

Figure 8 shows preliminary (averaging over 30 initial distributions of mode phases and energies) calculations of vibrational lifetimes at T=130 K for four modes: a C-related SLM at 556 cm^{-1} associated with the Si/C interface (Fig. 2);

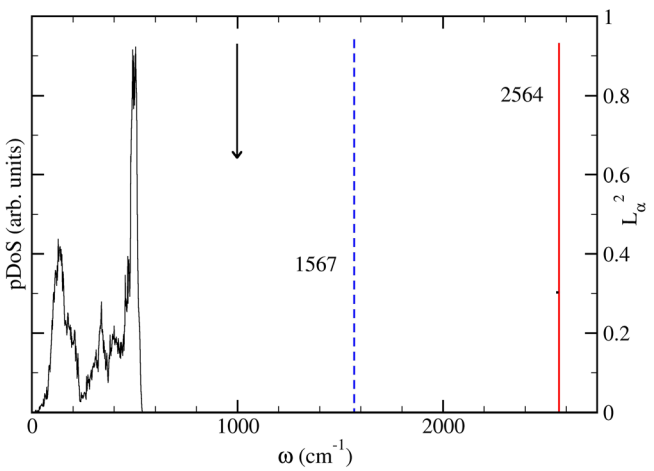

FIG. 7. Calculated pDoS of Si (left scale) and localization (right scale) of the H_{ab}–C stretch mode at 2 564 cm^{-1} and of the receiving D_{bc}–Si stretch mode at 1 567 cm^{-1}. The arrow points to $\Delta\omega$, with $\hbar\omega(H_{ab}\text{-}C) = \hbar\omega(D_{bc}\text{-}Si) + \hbar\Delta\omega$.

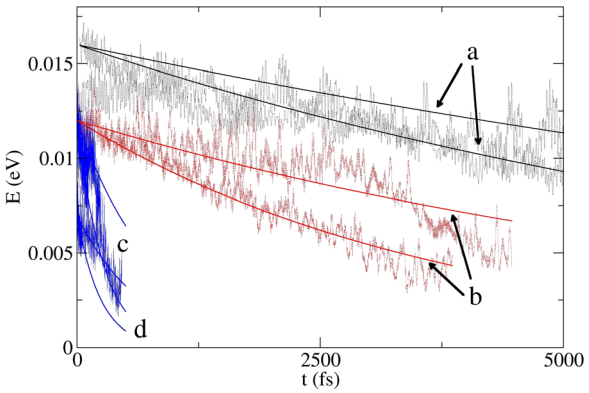

FIG. 8. Calculated vibrational lifetimes at 130 K of (a) a C-related SLM at 556 cm^{-1}, (b) a Ge-related SLM at 426 cm^{-1}, and (c) and (d) bulk modes at 424 and 241 cm^{-1}.

a Ge-related LVM at 426 cm^{-1} associated with the Si/Ge interface (Fig. 3); two bulk phonons (in a Si nanowire without δ layer) at 424 (intentionally close to the Ge-related mode) and 241 cm^{-1}, respectively.

In each case, two (or more) decay channels exist. The vibrational lifetimes are 10.5 and 17.2 ps for the C-related SLM at 556 cm^{-1} (a); 3.5 and 6.8 ps for the Ge-related SLM at 426 cm^{-1} (b); 0.3 and 0.8 ps for the bulk mode at 424 cm^{-1} (c); 0.2 and 0.6 ps for the bulk mode at 241 cm^{-1} (d). Thus, low-frequency SLMs trap phonons for lengths of time that are at least 5 and as much as 80 times longer than bulk modes.

The periods of these modes are 0.06, 0.08, 0.08, and 0.14 ps, respectively. Thus, the number of oscillations before decay is of the order of 167–300 for the C-related SLM and 50–87 for the Ge-related SLM. By the time it decays, the trapped phonon has lost all memory of the excitation that generated it. On the other hand, a phonon in a bulk mode decays after only a few oscillations.

V. ATOMISTIC DESCRIPTION OF PHONON SCATTERING AT DEFECTS

At low and moderate temperatures, high-frequency SLMs can only be excited optically. However, as shown in Sec. III, most defects also create low-frequency SLMs which can be excited thermally (Figs. 2 and 3). When a temperature gradient is applied, bulk phonons propagate from the warmer to the colder parts of the crystal until thermal equilibrium is established.

The interactions of propagating bulk phonons with defect-related SLMs are traditionally described using the empirical concept of (bulk) phonon scattering, first introduced by Peierls in 1929 (Ref. 22) and further refined by Klemens, Ziman, and Callaway.[23–25] In this description, defects play a purely static role as scattering centers for bulk phonons, and the defect-related SLMs are ignored. Callaway[25] introduced a range of parameters within the Boltzmann transport equation in order to model the time τ between scattering events for bulk phonons: $1/\tau = 1/\tau_n + 1/\tau_U + 1/\tau_{gb} + 1/\tau_i +$., where n, U, gb, and i, refer to normal, Umklapp, grain boundary, and impurity scattering, respectively. This approach is used by many authors to

describe (bulk) phonon scattering by point defects,[26–28] boundaries,[26–30] alloys,[29] surfaces,[31] etc.

Phonon scattering by defects can be visualized as follows. If the warmer bulk phonons are a wave propagating on a body of water, then a defect is a rock in its path. This rock locally scatters the water wave and thus slows down the flow of water. Different types of defects correspond to rocks of different shapes and sizes.

At the atomic scale, the scattering of bulk phonons is more subtle. In the higher-T region, there are more low-frequency bulk phonons and higher-frequency phonons than in the lower-T region. When encountering a defect, the warmer bulk phonons displace the atoms making up the defect and thus excite some of the defect-related SLMs. These excitations remain localized for a length of time equal to their vibrational lifetime, and then undergo a (normal or anomalous) decay into a combination of bulk phonons with frequency lower than that of the excited SLM.

Thus, phonon scattering by defects is phonon trapping by the defect followed by the decay of the excitation into lower-frequency bulk phonons. The water-wave-scattered-by-a-rock analogy needs to be refined. The rock behaves like a sponge. It absorbs a little bit of the incoming water and ultimately releases it, but the time scale involved depends on the defect and sometimes on its isotopic composition.

We illustrate this with a mono-atomic δ-layer of Ge in a Si nanowire. There are no Ge-Ge modes but the low-frequency Si-Ge modes are localized. They trap thermal phonons and this impedes the flow of heat. In this calculation, we used a H-terminated Si nanowire with 1D periodic boundary conditions and two symmetrically located mono-atomic δ-layers of Ge (Fig. 9).

A thin Si layer on the left was prepared at $T_{hot} = 270\,K$ and the rest of the nanowire at $T_{cold} = 115\,K$. The final temperature is $T_{avg} = 125\,K$. The temperature vs. time in the central slice was recorded for 100 MD simulations with different initial random mode phases and energies. Figure 10 compares T(t) in the central slice calculated without and with the δ-layer. Without the δ-layer, the central slice reaches its final temperature after about 5 ps, leading to a calculated thermal conductivity $\kappa = 0.22\,W/mK$. With the δ-layer, the central slice reaches T_{avg} after about 12 ps, and the thermal conductivity drops to 0.08 W/mK. The substantial ~7 ps delay is caused by phonon trapping at the SLMs associated with the Ge δ-layer. The temperature of the δ-layer remains above T_{avg} for the length of the MD simulation, consistent with phonon trapping. More details on this will be published elsewhere.[32]

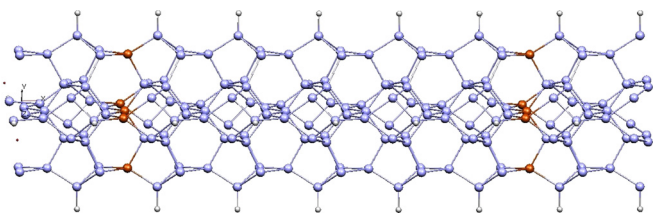

FIG. 9. H-terminated Si nanowire with 1D periodic boundary conditions. Two mono-atomic δ-layer of Ge (5 Ge atoms each) are symmetrically located on either side of the central slices where T(t) is recorded.

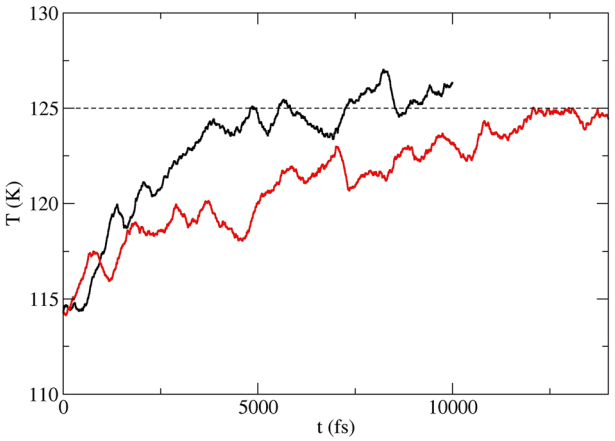

FIG. 10. Temperature vs. time in the central slice without (black curve, top) and with (red curve, bottom) a mono-atomic δ-layer of Ge (Fig. 9). The central slice reaches the final temperature after ~5 ps without δ-layer and after ~12 ps with the δ-layer. The time step is 1 fs.

VI. HEAT FLOW AT A HETEROJUNCTION: THE ROLE OF THE INTERFACE SLMS

Phonon trapping and the decay of the vibrational excitations are critical to understand the flow of heat at the interface between two materials, such as Si/Ge or Si/C. The simplified situation discussed here is a 4-atom-thick Ge or C δ-layer in a Si nanowire (Fig. 11). The interface of the Ge (C) δ-layer introduces SLMs with lower- (higher-) frequencies than Si-related modes (Figs. 2 and 3).

We establish a T gradient by preparing a thin layer of Si atoms at the temperature $T_{hot} = 520\,K$, on the far left side of the nanowire, while the rest (including the δ-layer) is in thermal equilibrium at $T_{cold} = 120K$. The final (equilibrium) temperature is $T_{avg} = 140\,K$.

As the MD runs progress, we monitor the temperature along the nanowire. Some of the SLMs at the interface trap phonons and, after some time, these excitations decay into bulk phonons of *lower* frequency. However, there are far fewer low-frequency receiving phonons on the C side of the Si/C system (Fig. 2) than on the Ge side of the Si/Ge system (Fig. 3). As a result, most of the heat propagates readily into the Ge δ-layer but bounces off the C δ-layer.

Figure 12 compares (preliminary calculations) the temperature at the Si-Ge and the Si-C interfaces. In the case of Si-Ge, the temperature promptly increases from $T_{cold} = 120\,K$ to $T_{avg} = 140\,K$. The phonons trapped at the interface SLMs decay primarily into the low-frequency Ge modes (to the right of the interface), leading to a high coefficient of transmission. On the other hand, the temperature of the Si-C layer slowly increases from 120 K to 130 K, because the phonons trapped at the interface SLMs decay back into Si bulk phonons (to the left of the interface), leading to a high coefficient of reflection. Detailed calculations are under way.[18]

Optical experiments[33] on crystalline Si nanodots in a SiO_2 matrix have revealed that the nanodots melt (become amorphous) upon laser excitations at power levels far below the expected melting threshold. This was interpreted as being related to the very low thermal conductivity in the nanodots. However, something else may be at play. The laser-generated

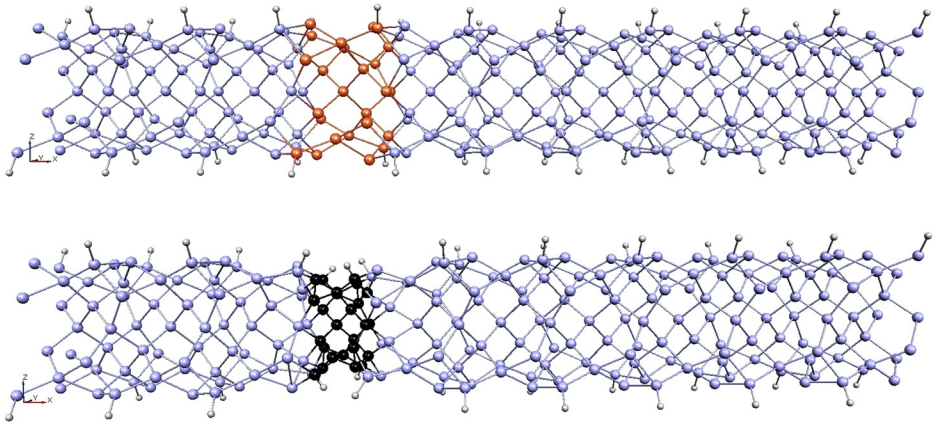

FIG. 11. H-saturated 1D periodic Si nanowires $Si_{225}X_{25}H_{40}$ with a 4-atom-thick δ-layer of X = Ge (top) or X = C (bottom).

vibrational excitations in the Si nanodots decay into lower-frequency bulk Si modes which propagate toward the interface with SiO_2. Most of the heat is reflected because most Si-O bonds have much higher frequencies than Si-Si bonds and thus provide few low-frequency receiving modes. Further, any heat in the SiO_2 matrix easily diffuses into the Si nanodots—but not out of them, for the same reason. Thus, almost all the heat generated by the laser excitation (in the Si nanodots as well as in the neighboring SiO_2 matrix) traps in the nanodots.

One might repeat the experiment with a matrix of atoms heavier than Si (such as a Ge matrix) as most of the heat injected by the laser beam in a Si nanodots would flow into the lower-frequency modes of the matrix instead of being reflected back into the Si, while the heat generated in the matrix would mostly bounce back into the matrix at the matrix-nanodot interface.

VII. SUMMARY AND OUTLOOK

This paper focused on the spatially localized high- and low-frequency vibrational modes associated with defects in crystalline semiconductors and semiconductor nanostructures. These modes often exhibit a high degree of localization and trap (optical or thermal) phonons for some length of time before decaying into lower-frequency bulk phonons. Measurements and calculations of the vibrational lifetimes of optically-excited high-frequency LVMs show that two types of decay must be distinguished: *normal*—which involves only bulk phonons and obeys conventional theory,[10,11] and *anomalous*—which involves other defect-related SLMs, does not obey conventional theory, and sometimes exhibit very large isotope effects.

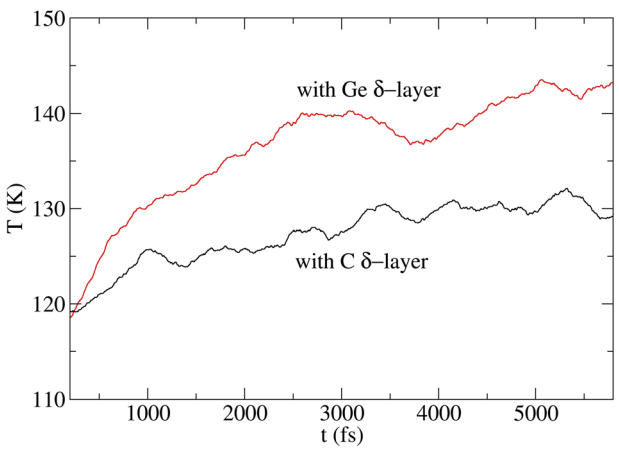

FIG. 12. Running average of the temperature (K) vs. time (fs) of the Si-Ge (red, top) and Si-C (black, bottom) interfaces for a 4-atom thick δ-layer in a Si nanowire (Fig. 11). The initial and final (equilibrium) temperatures are 120K and 140 K, respectively.

Theory predicts that all defects introduce SLMs. Their *localization* can be quantified using the eigenvectors of the dynamical matrix. Many of these modes can trap thermal phonons. This becomes important when the concentration of defects is (locally) high. The conventional description of the impact of defects on the flow of heat involves the empirical concept of (bulk) phonon scattering, in which defects are static scattering centers. This description works well when the concentration of defects is low. At the atomic level, bulk phonon scattering involves the vibrational properties of the defect: SLMs trap phonons for a length of time which is defect-dependent, and then the excitation decays into bulk phonons of lower-frequency. Thus, the vibrational dynamics of defects are important, and *phonon trapping* cannot be ignored for extended defects such as interfaces or in nanostructures.

If we add one phonon to bulk vibrational modes, the decay occurs within a few periods of oscillation. But SLMs of similar frequency typically trap phonons for dozens or even hundreds of periods of oscillation. Phonon trapping occurs at impurities, dislocations, grain boundaries, interfaces, surfaces, and other defects. The vibrational lifetimes of SLMs vary with the defect and sometimes its isotopic composition, which suggests that defect engineering of heat flow is in principle possible.

One application discussed here involves the interaction of a flow of heat with a Si/C or Si/Ge interface. The heat trapped at the interface-related SLMs can only decay into lower-frequency modes, therefore mostly on the Si side of the Si/C interface (large coefficient of reflection) and mostly on the Ge side of the Si/Ge interface (large coefficient of transmission). This provides a possible explanation as to why crystalline Si nanodots in a SiO_x matrix become amorphous following exposure to light. This also suggests the possibility of engineering thermal "devices".[34] For example, phonons could be trapped between two δ-layers (or within a

single thick δ-layer) in a Si nanowire. Such a configuration would be analogous to the trapping photons between two mirrors in a laser.[35]

Thus, it might be possible to engineer the flow of heat in semiconductors and nanostructures, either by doping with specific (isotopes of) impurities or by playing with coefficients of reflection and transmission at various interfaces or in superlattices.

ACKNOWLEDGMENTS

The work of S.K.E. was supported in part by the Grant No. D-1126 from the R. A. Welch Foundation. The authors are thankful to Texas Tech's High-Performance Computer Center for generous amounts of CPU time.

[1]M. Stavola, in *Hydrogen in Crystalline Semiconductors*, edited by S. J. Pearton, J. W. Corbett, and M. Stavola (Springer-Verlag, Berlin, 1991), p. 102.
[2]B. Pajot, in *Oxygen in Semiconductors*, edited by F. Shimura (Academic, Boston, 1994), p. 161.
[3]M. Steger, A. Yang, T. Sekiguchi, K. Saeedi, M. L. W. Thewalt, M. O. Henry, K. Johnston, H. Riemann, N. V. Abrosimov, M. F. Churbanov, A. V. Gusev, A. K. Kaliteevskii, O. N. Godisov, P. Becker, and H.-J. Pohl, J. Appl. Phys. **110**, 081301 (2011).
[4]A. Carvalho, D. J. Backlund, and S. K. Estreicher, Phys. Rev. B **84**, 155322 (2011).
[5]G. Lüpke, N. H. Tolk, and L. C. Feldman, J. Appl. Phys. **93**, 2317 (2003).
[6]G. Lüpke, X. Zhang, B. Sun, A. Fraser, N. H. Tolk, and L. C. Feldman, Phys. Rev. Lett. **88**, 135501 (2002).
[7]K. K. Kohli, G. Davies, N. Q. Vinh, D. West, S. K. Estreicher, T. Gregorkiewicz, and K. M. Itoh, Phys. Rev. Lett. **96**, 225503 (2006).
[8]T. M. Gibbons, S. K. Estreicher, K. Potter, F. Bekisli, and M. Stavola, Phys. Rev. B **87**, 115207 (2013).
[9]D. West and S. K. Estreicher, Phys. Rev. Lett. **96**, 115504 (2006); Phys. Rev. B **75**, 075206 (2007).
[10]A. Nitzan and J. Jortner, Mol. Phys. **25**, 713 (1973); A. Nitzan, S. Mukamel, and J. Jortner, J. Chem. Phys. **60**, 3929 (1974).
[11]S. A. Egorov and J. L. Skinner, J. Chem. Phys. **103**, 1533 (1995).
[12]M. Cardona and M. L. W. Thewalt, Rev. Mod. Phys. **77**, 1173 (2005).
[13]*Theory of Defects in Semiconductors, Topics in Applied Physics Vol. 104*, edited by D. A. Drabold and S. K. Estreicher (Springer, Heidelberg, 2007).
[14]H. Hellmann, *Einführung in Die Quantenchemie* (Franz Deuticke, Leipzig, 1937), p. 285; R. P. Feynman, Phys. Rev. **56**, 340 (1939).
[15]D. Sánchez-Portal, P. Ordejón, E. Artacho, and J. M. Soler, Int. J. Quantum Chem. **65**, 453 (1997); E. Artacho, D. Sánchez-Portal, P. Ordejón, A. García, and J. M. Soler, Phys. Status Solidi B **215**, 809 (1999).
[16]T. M. Gibbons, By. Kang, S. K. Estreicher, and C. Carbogno, Phys. Rev. B **84**, 035317 (2011).
[17]This use of the eigenvectors of the dynamical matrix was proposed in S. K. Estreicher, D. West, J. Goss, S. Knack, and J. Weber, Phys. Rev. Lett. **90**, 035504 (2003).
[18]M. B. Bebek, private communication (2013).
[19]G. Davies first mentioned phonon trapping in a lecture at the 25th International Conference on Defects in Semiconductors (St. Petersburg, 2009).
[20]M. Stavola, private communication (2013).
[21]T. M. Gibbons and S. K. Estreicher, (unpublished).
[22]R. Peierls, Ann. Phys. **395**, 1055 (1929).
[23]P. G. Klemens, Proc. Phys. Soc. A **68**, 1113 (1955); P. G. Klemens, *Solid State Physics: Advances and Applications*, edited by F. Seitz and D. Turnbull (Academic, New York, 1988), Vol. 7.
[24]J. M. Ziman, *Electrons and Phonons* (Oxford, Clarendon, 1960), pp. 220–223.
[25]J. Callaway, Phys. Rev. **113**, 1046 (1959).
[26]D. A. Broido, M. Malorny, G. Birner, N. Mingo, and D. A. Stewart, Appl. Phys. Lett. **91**, 231922 (2007).
[27]M. Kazan, G. Guisbiers, S. Pereira, M. R. Correia, P. Masri, A. Bruyant, S. Volz, and P. Royer, J. Appl. Phys. **107**, 083503 (2010).
[28]A. Sparavigna, Phys. Rev. B **67**, 144305 (2003).
[29]Z. Wang and N. Mingo, Appl. Phys. Lett. **97**, 101903 (2010).
[30]M. Maldovan, J. Appl. Phys. **111**, 024311 (2012).
[31]P. Martin, A. Aksamifa, E. Pop, and U. Ravaioli, Phys. Rev. Lett. **102**, 125503 (2009).
[32]By. Kang and S. K. Estreicher, (unpublished).
[33]B. V. Kamenev, H. Grabel, and L. Tsybeskov, Appl. Phys. Lett. **88**, 143117 (2006).
[34]N. Li, J. Ren, L. Wang, G. Zhang, P. Hänggi, and B. Li, Rev. Mod. Phys. **84**, 1045 (2012).
[35]L. Grave-de-Peralta, private communication (2013).